



## Origin of the material dependence of $T_c$ in the single-layered cuprates

Hirofumi Sakakibara,<sup>1</sup> Hidetomo Usui,<sup>2</sup> Kazuhiko Kuroki,<sup>1,5</sup> Ryotaro Arita,<sup>3,5,6</sup> and Hideo Aoki<sup>4,5</sup>

<sup>1</sup>*Department of Engineering Science, The University of Electro-Communications, Chofu, Tokyo 182-8585, Japan*

<sup>2</sup>*Department of Applied Physics and Chemistry, The University of Electro-Communications, Chofu, Tokyo 182-8585, Japan*

<sup>3</sup>*Department of Applied Physics, The University of Tokyo, Hongo, Tokyo 113-8656, Japan*

<sup>4</sup>*Department of Physics, The University of Tokyo, Hongo, Tokyo 113-0033, Japan*

<sup>5</sup>*JST, TRIP, Sanbancho, Chiyoda, Tokyo 102-0075, Japan*

<sup>6</sup>*JST, PRESTO, Kawaguchi, Saitama 332-0012, Japan*

(Received 5 December 2011; published 1 February 2012)

In order to understand the material dependence of  $T_c$  within the single-layered cuprates, we study a two-orbital model that considers both  $d_{x^2-y^2}$  and  $d_{z^2}$  orbitals. We reveal that a hybridization of  $d_{z^2}$  on the Fermi surface substantially affects  $T_c$  in the cuprates, where the energy difference  $\Delta E$  between the  $d_{x^2-y^2}$  and the  $d_{z^2}$  orbitals is identified to be the key parameter that governs both the hybridization and the shape of the Fermi surface. A smaller  $\Delta E$  tends to suppress  $T_c$  through a larger hybridization, whose effect supersedes the effect of diamond-shaped (better-nested) Fermi surface. The mechanism of the suppression of  $d$ -wave superconductivity due to  $d_{z^2}$  orbital mixture is clarified from the viewpoint of the ingredients involved in the Eliashberg equation, that is, the Green's functions and the form of the pairing interaction described in the orbital representation. The conclusion remains qualitatively the same if we take a three-orbital model that incorporates the Cu  $4s$  orbital explicitly, where the  $4s$  orbital is shown to have an important effect of making the Fermi surface rounded. We have then identified the origin of the material and lattice-structure dependence of  $\Delta E$ , which is shown to be determined by the energy difference  $\Delta E_d$  between the two Cu  $3d$  orbitals (primarily governed by the apical oxygen height) and the energy difference  $\Delta E_p$  between the in-plane and apical oxygens (primarily governed by the interlayer separation  $d$ ).

DOI: [10.1103/PhysRevB.85.064501](https://doi.org/10.1103/PhysRevB.85.064501)

PACS number(s): 74.20.-z, 74.62.Bf, 74.72.-h

### I. INTRODUCTION

Despite the fact that the history of the high- $T_c$  cuprates exceeds two decades, there remain a number of fundamental questions which are yet to be resolved. Among them is the significant variation of  $T_c$  among various materials within the cuprate family. It is well known that  $T_c$  varies strongly with the number of  $\text{CuO}_2$  layers, but an even more basic problem is the  $T_c$  variation within the single-layered materials. This is highlighted by  $\text{La}_{2-x}(\text{Sr/Ba})_x\text{CuO}_4$  with a  $T_c \simeq 40$  K versus  $\text{HgBa}_2\text{CuO}_{4+\delta}$  with a  $T_c \simeq 90$  K, with a more than factor of two difference despite similar crystal structures between them.

Empirically, it has been recognized that the materials with  $T_c \sim 100$  K tend to have “round” Fermi surfaces, while the Fermi surface of the La system is closer to a diamond shape, and this has posed a long-standing, big puzzle, since the latter would imply a relatively better nesting.<sup>1,2</sup> The materials with rounded Fermi surfaces conventionally have been analyzed with a single-band model with large second [ $t_2(>0)$ ] and third [ $t_3(<0)$ ] neighbor hopping integrals, while the “low- $T_c$ ” La system has been considered to have smaller  $t_2, t_3$ . This, however, has brought about a contradiction between theories and experiments. Namely, while some phenomenological<sup>3</sup> and  $t$ - $J$  model<sup>4,5</sup> studies give a tendency consistent with the experiments, a number of many-body approaches for the *Hubbard-type* models with realistic values of on-site interaction  $U$  show suppression of superconductivity for large  $t_2 > 0$  and/or  $t_3 < 0$ , as we indeed confirm below.<sup>6</sup>

To resolve this discrepancy, we have introduced in Ref. 7 a two-orbital model that explicitly incorporates the  $d_{z^2}$  orbital as well, while the usual wisdom was that the  $d_{x^2-y^2}$  orbital suffices. The former component has, in fact, a significant contribution to the Fermi surface in the La system. We

have shown that the key parameter that determines  $T_c$  is the hybridization of the two orbitals, which is, in turn, governed by the level offset  $\Delta E$  between the  $d_{x^2-y^2}$  and the  $d_{z^2}$  Wannier orbitals. Namely, the weaker the  $d_{z^2}$  contribution to the Fermi surface, the better it is for  $d$ -wave superconductivity, where a weaker contribution of the  $d_{z^2}$  results in a rounded Fermi surface (which in itself is not desirable for superconductivity), but it is the “single-orbital nature” that favors a higher  $T_c$  superseding the effect of the Fermi surface shape. Recently, there have also been some other theoretical studies regarding the role of the  $d_{z^2}$  orbital played in the cuprates.<sup>8-11</sup>

The purpose of the present paper is twofold: By elaborating the two-orbital model, we investigate (i) why the  $d_{z^2}$  hybridization on the Fermi surface suppresses the superconductivity, and (ii) what are the key components that determine the material dependence in the level offset between  $d_{x^2-y^2}$  and  $d_{z^2}$ . In examining point (ii), in addition to  $\text{La}_2\text{CuO}_4$  and  $\text{HgBa}_2\text{CuO}_{4+\delta}$  considered in Ref. 7, we also construct effective models of the single-layered cuprates  $\text{Bi}_2\text{Sr}_2\text{CuO}_6$  and  $\text{Tl}_2\text{Ba}_2\text{CuO}_6$  to reveal how these materials can be classified in terms of the correlation between the lattice structure parameters and the level offsets of various orbits.

### II. CONSTRUCTION OF THE TWO-ORBITAL MODEL

#### A. Band calculation

Let us start with the first-principles band calculation<sup>12</sup> of  $\text{La}_2\text{CuO}_4$  and  $\text{HgBa}_2\text{CuO}_4$ , whose band structures are displayed in Fig. 1. The lattice parameters adopted here are experimentally determined ones for the doped materials.<sup>13,14</sup> In both cases, there is only one band intersecting the Fermi level. Therefore, the  $d_{x^2-y^2}$  single-orbital Hubbard model, or

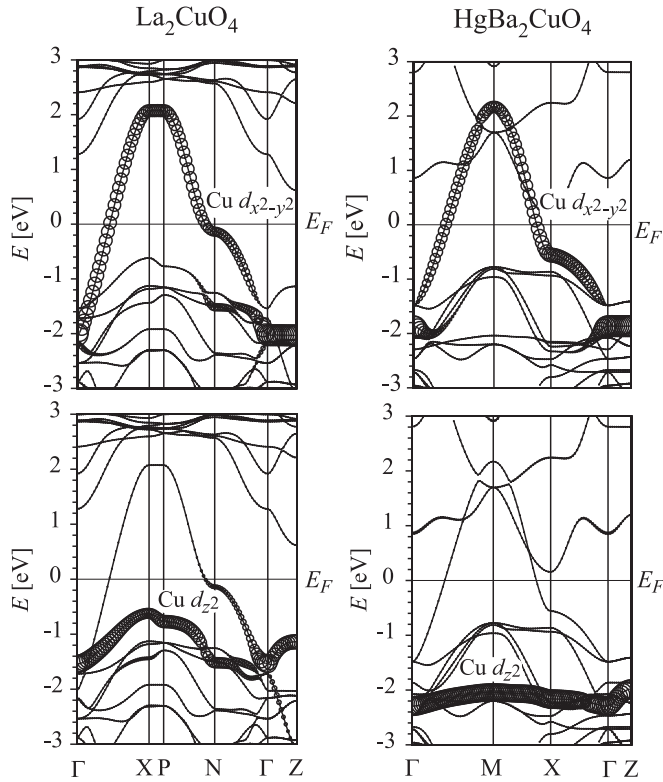


FIG. 1. First-principles band structures of  $\text{La}_2\text{CuO}_4$  (left) and  $\text{HgBa}_2\text{CuO}_4$  (right). The top (bottom) panels depict the strength of the  $d_{x^2-y^2}$  ( $d_{z^2}$ ) characters with the radius of the circles.

the  $\text{Cu-}d_{x^2-y^2} + \text{O-}p_\sigma$  three-orbital model (whose antibonding band crosses the Fermi level) has been adopted in conventional theoretical studies. A large difference between the two materials in the shape of the Fermi surface is confirmed in Fig. 2. As mentioned in the Introduction, the materials with a rounded Fermi surface have been modeled by a single-orbital model with large second [ $t_2(>0)$ ] and third [ $t_3(<0)$ ] neighbor hopping integrals.<sup>1</sup> It has been noticed that when the fluctuation exchange (FLEX) approximation<sup>15,16</sup> is applied to this model, a rounder Fermi surface coming from larger second- and third-neighbor hoppings results in a suppressed  $T_c$ , as we have shown in Fig. 1 of Ref. 7. A calculation with the dynamical cluster approximation (DCA) shows that a negative  $t_2$  works destructively against  $d$ -wave superconductivity,<sup>17</sup> and

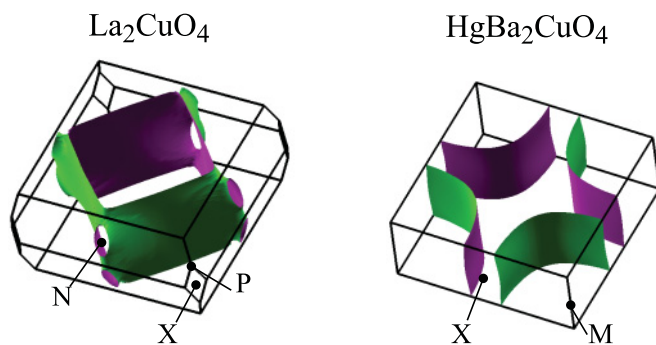


FIG. 2. (Color online) The Fermi surface of the  $\text{La}_2\text{CuO}_4$  (left) and  $\text{HgBa}_2\text{CuO}_4$  (right) with 0.15 holes/Cu atom.

a more realistic DCA calculation that considers the oxygen  $p_\sigma$  orbitals for the La and Hg cuprates also indicates a similar tendency.<sup>18</sup>

## B. The two-orbital model

To resolve the above problem for the  $d_{x^2-y^2}$  single-orbital model, we now focus on other orbital degrees of freedom. In fact, Fig. 1 shows that in the La system the main band has a strong  $d_{z^2}$  character around the N point on the Fermi surface that corresponds to the wave vectors  $(\pi, 0), (0, \pi)$  in a square lattice. This has been recognized from an early stage of the study on the cuprates,<sup>19–22</sup> and more recently, it has been discussed in Refs. 23 and 1 that the mixture of  $d_{z^2}$  character to the main component determines the shape of the Fermi surface. Namely, the large  $d_{z^2}$  contribution in the La system makes the Fermi surface closer to a square (i.e., a diamond), while in the Hg cuprate the  $d_{z^2}$  contribution is small and the Fermi surface is more rounded (as confirmed in the following).

In order to understand the experimentally observed correlation between the Fermi surface shape and  $T_c$ , we consider a two-orbital model that takes into account not only the  $d_{x^2-y^2}$  Wannier orbital but also the  $d_{z^2}$  Wannier orbital explicitly.<sup>7</sup> A first-principles calculation<sup>12,24</sup> is used to construct maximally localized Wannier orbitals,<sup>25,26</sup> from which the hopping integrals and the on-site energies of the two-orbital tight-binding model for the La and Hg cuprates are deduced. Thus obtained band structures of the two-orbital model for the La and Hg cuprates are shown in Fig. 3, along with the Fermi surface for the band filling of  $n = 2.85$  ( $n =$  number of electrons per site), which corresponds to 0.15 holes per Cu atom.

In the present two-orbital model, the  $d_{x^2-y^2}$  Wannier orbital originates primarily from the Cu  $3d_{x^2-y^2}$  and the in-plane O  $2p_\sigma$  orbitals. On the other hand, the  $d_{z^2}$  Wannier orbital originates mainly from the Cu  $3d_{z^2}$  and apical O  $2p_z$  orbitals. Namely, this model incorporates two types of  $d$ - $p_\sigma$  antibonding states, where the former spreads over the  $\text{CuO}_2$  plane while the latter spreads along the  $c$  axis (Fig. 4). Table I shows the parameter values of the present model, from which we can identify that  $d_{x^2-y^2} - d_{z^2}$  interorbital hopping occurs mainly between nearest-neighbor Cu sites, which gives rise to the orbital mixture. Because the  $d_{x^2-y^2} - d_{z^2}$  hopping integrals are similar for the La and Hg compounds, the onsite energy difference  $\Delta E = E_{x^2-y^2} - E_{z^2}$  between the two orbitals can be used as a measure of the  $d_{z^2}$  mixture. Note that the interorbital hoppings have different signs between  $x$  and  $y$  directions, that is, the matrix element has the form  $-2t_1[\cos(k_x) - \cos(k_y)]$ , so that the  $d_{x^2-y^2} - d_{z^2}$  mixture is strong around the wave vectors  $(\pi, 0), (0, \pi)$  (N point in the La cuprate), while small around  $|k_x| = |k_y|$ .

In Table I we also show the parameters for the single-orbital model obtained by the similar method. In the single-orbital model, the “ $d_{x^2-y^2}$ ” Wannier orbital effectively contains the  $d_{z^2}$  orbital in the tail parts of the Wannier orbital.

## C. Correlation between the curvature of the Fermi surface and $\Delta E$

The  $d_{z^2}$  orbital contribution has also a large effect on the curvature of the Fermi surface,<sup>1,23</sup> which can indeed be seen

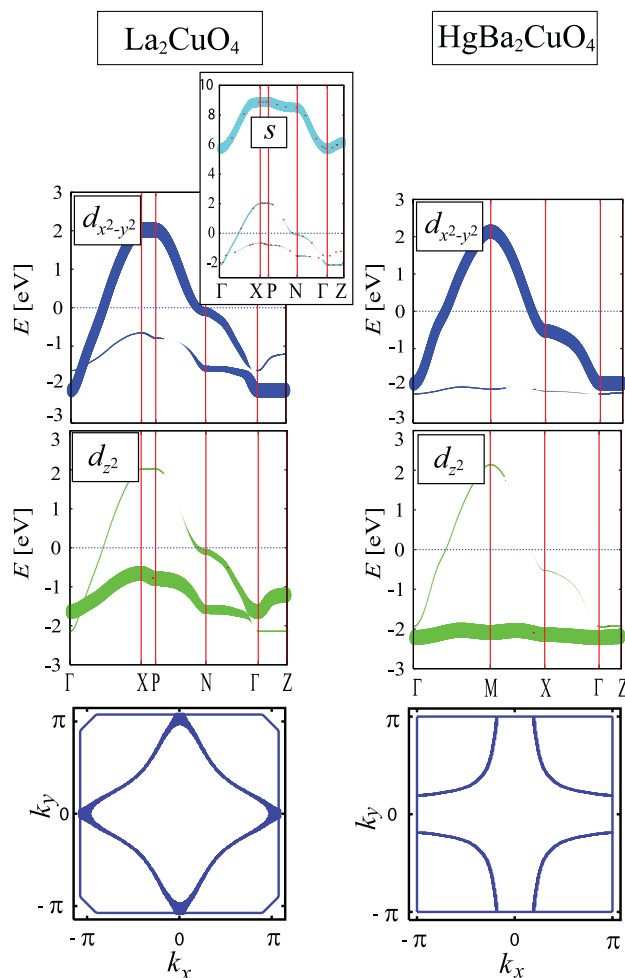


FIG. 3. (Color online) The band structure (with  $E_F = 0$ ) in the two-orbital ( $d_{x^2-y^2}$ - $d_{z^2}$ ) model for  $\text{La}_2\text{CuO}_4$  (left column) and  $\text{HgBa}_2\text{CuO}_4$  (right). The top (middle) panels depict the weights of the  $d_{x^2-y^2}$  ( $d_{z^2}$ ) characters with thickened lines, while the bottom panels are the Fermi surface for the band filling of  $n = 2.85$ . The inset shows the band structure of the three-orbital model (see text) for La system, where the  $4s$  character is indicated by thick lines.

from Table I as follows. In the single-orbital model, the La cuprate has smaller  $t_2$  and  $t_3$  as compared to the Hg cuprate

TABLE I. Hopping integrals within the  $d_{x^2-y^2}$  orbital for the single- and two-orbital models (upper half), interorbital hopping (middle), and  $\Delta E \equiv E_{d_{x^2-y^2}} - E_{d_{z^2}}$  (bottom).

	One-orbital		Two-orbital	
	La	Hg	La	Hg
$t(d_{x^2-y^2} \rightarrow d_{x^2-y^2})$				
$t_1$ (eV)	-0.444	-0.453	-0.471	-0.456
$t_2$ (eV)	0.0284	0.0874	0.0932	0.0993
$t_3$ (eV)	-0.0357	-0.0825	-0.0734	-0.0897
$( t_2  +  t_3 )/ t_1 $	0.14	0.37	0.35	0.41
$t(d_{x^2-y^2} \rightarrow d_{z^2})$				
$t_1$ (eV)			0.178	0.105
$t_2$ (eV)			Small	Small
$t_3$ (eV)			0.0258	0.0149
$\Delta E$ (eV)			0.91	2.19

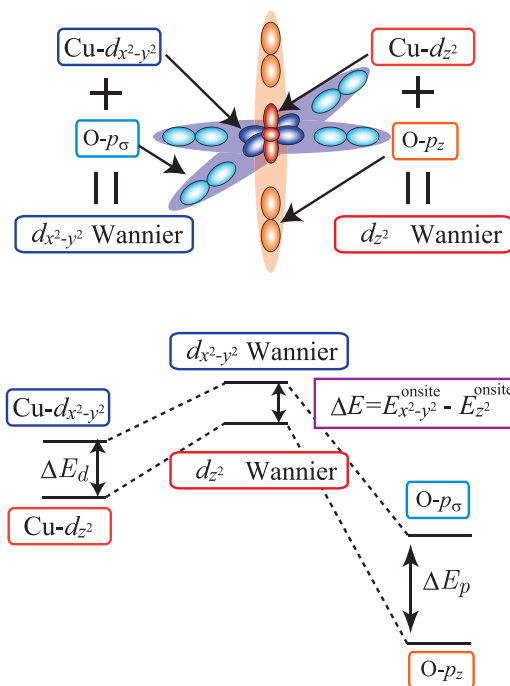


FIG. 4. (Color online) The top panel shows the main components of the two Wannier orbitals (having different types of  $\sigma$  bonding) considered in the present two-orbital model. The bottom panel shows the schematic definition of the level offsets  $\Delta E$ ,  $\Delta E_d$ , and  $\Delta E_p$ .

[with the ratio  $(|t_2| + |t_3|)/|t_1|$  being 0.14 (0.37) for La (Hg)], resulting in the smaller curvature of the Fermi surface in the former as mentioned. On the other hand, in the two-orbital model that considers the  $d_{z^2}$  orbital explicitly, the ratio  $(|t_2| + |t_3|)/|t_1|$  within the  $d_{x^2-y^2}$  orbital changes to 0.35 (0.41) for the La (Hg). The value is nearly the same between the single- and two-orbital modeling of Hg, while the value is significantly increased in the two-orbital model for La. The reason why  $t_2$  and  $t_3$  in the two-orbital model for La are large as compared to those in the single-orbital model can be understood from Fig. 5 as follows. Let us consider the diagonal hopping ( $t_2$ ). There is a direct ( $d_{x^2-y^2} - d_{x^2-y^2}$ ) diagonal hopping, but there is also an indirect diagonal hopping that becomes effective when  $\Delta E$  is small, that is,  $d_{x^2-y^2} \rightarrow d_{z^2} \rightarrow d_{x^2-y^2}$ . In the single-orbital model, where the  $d_{z^2}$  component is effectively included in the  $d_{x^2-y^2}$  Wannier orbital, the contribution of the  $d_{x^2-y^2} \rightarrow d_{z^2} \rightarrow d_{x^2-y^2}$  path is effectively included in  $t_2$ . The latter contribution has a sign opposite that of the direct diagonal hopping (the reason for which is clarified later), so that we end up with a small effective  $t_2$  in the single-orbital model when  $\Delta E$  is small as in the La cuprate. A similar argument applies to  $t_3$ . Conversely, the Hg cuprate has a large  $\Delta E$  so that the  $d_{z^2}$  contribution barely exists in the single-orbital model, and the ratio  $(|t_2| + |t_3|)/|t_1|$  is similar to that in the two-orbital model.

In the La cuprate, the  $d_{x^2-y^2}$  and  $d_{z^2}$  orbitals strongly mix around the N point, so that the upper and lower bands repel each other there, and the saddle point of the upper band that corresponds to the van Hove singularity is pushed up to nearly touch the Fermi level for the band filling of  $n = 2.85$ . Thus, the Fermi surface almost touches the wave vectors  $(\pi, 0)$ ,  $(0, \pi)$ . In the Hg cuprate, there is no such splitting of the two bands, and

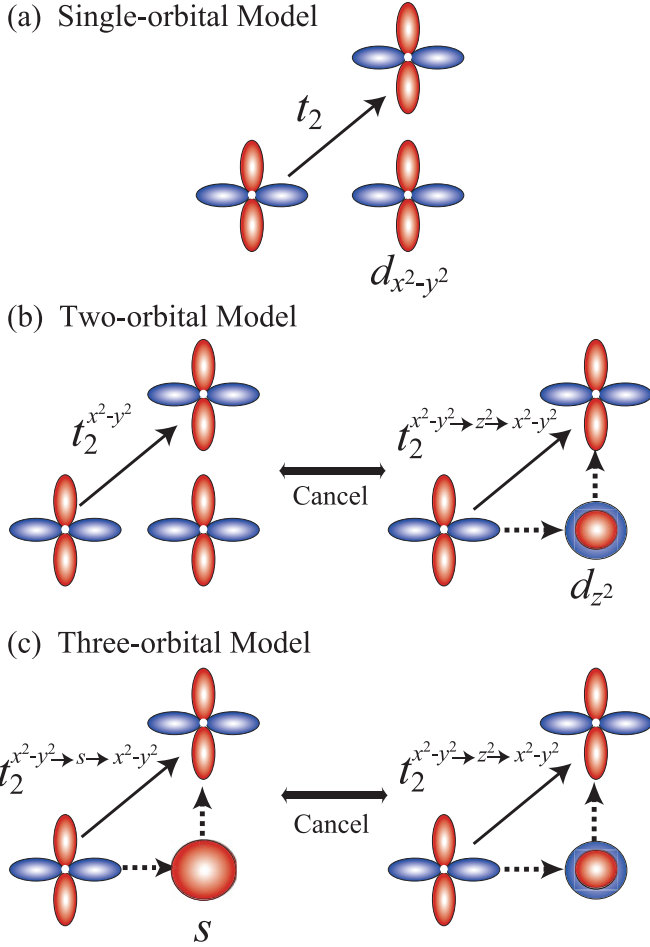


FIG. 5. (Color online) Origin of the effective second-neighbor hopping [ $t_2$  in the single-band model, (a) in the two-orbital (b) and three-orbital (c) models.

the saddle point stays well below the Fermi level, resulting in a rounded Fermi surface that is closed around the wave vector  $(\pi, \pi)$ .

### III. MANY-BODY CALCULATION OF THE SUPERCONDUCTIVITY

#### A. Calculation method

We now consider a many-body Hamiltonian based on the two-orbital tight-binding model discussed above, which is given, in the standard notation, as

$$\begin{aligned}
 H = & \sum_i \sum_{\mu} \sum_{\sigma} \varepsilon_{\mu} n_{i\mu\sigma} + \sum_{ij} \sum_{\mu\nu} \sum_{\sigma} t_{ij}^{\mu\nu} c_{i\mu\sigma}^{\dagger} c_{j\nu\sigma} \\
 & + \sum_i \left( U \sum_{\mu} n_{i\mu\uparrow} n_{i\mu\downarrow} + U' \sum_{\mu>\nu} \sum_{\sigma, \sigma'} n_{i\mu\sigma} n_{i\nu\sigma'} \right. \\
 & - \frac{J}{2} \sum_{\mu \neq \nu} \sum_{\sigma, \sigma'} c_{i\mu\sigma}^{\dagger} c_{i\mu\sigma'} c_{i\nu\sigma'}^{\dagger} c_{i\nu\sigma} \\
 & \left. + J' \sum_{\mu \neq \nu} c_{i\mu\uparrow}^{\dagger} c_{i\mu\downarrow}^{\dagger} c_{i\nu\downarrow} c_{i\nu\uparrow} \right), \quad (1)
 \end{aligned}$$

where  $i, j$  denote the sites and  $\mu, \nu$  the two-orbitals, while the electron-electron interactions comprise the intraorbital repulsion  $U$ , interorbital repulsion  $U'$ , and the Hund's coupling  $J$  (= pair-hopping interaction  $J'$ ). Here we take  $U = 3.0$  eV,  $U' = 2.4$  eV, and  $J = 0.3$  eV.<sup>27</sup> These values conform to a widely accepted, first-principles estimations for the cuprates that the  $U$  is  $7t-10t$  (with  $t \simeq 0.45$  eV), while  $J, J' \simeq 0.1U$ . Here we also observe the orbital SU(2) requirement  $U' = U - 2J$ .

To study the superconductivity in this multiorbital Hubbard model, we apply the FLEX approximation.<sup>15,16,28</sup> In FLEX, we start with the Dyson's equation to obtain the renormalized Green's function, which, in the multiorbital case, is a matrix in the orbital representation as  $G_{l_1 l_2}$ , where  $l_1$  and  $l_2$  are orbital indices. The bubble and ladder diagrams consisting of the renormalized Green's function are then summed to obtain the spin and charge susceptibilities,

$$\hat{\chi}_s(q) = \frac{\hat{\chi}^0(q)}{1 - \hat{S} \hat{\chi}^0(q)}, \quad (2)$$

$$\hat{\chi}_c(q) = \frac{\hat{\chi}^0(q)}{1 + \hat{C} \hat{\chi}^0(q)}, \quad (3)$$

where  $q \equiv (\vec{q}, i\omega_n)$  and the irreducible susceptibility is

$$\chi_{l_1, l_2, l_3, l_4}^0(q) = \sum_q G_{l_1 l_3}(k+q) G_{l_4 l_2}(k), \quad (4)$$

with the interaction matrices

$$S_{l_1 l_2, l_3 l_4} = \begin{cases} U, & l_1 = l_2 = l_3 = l_4, \\ U', & l_1 = l_3 \neq l_2 = l_4, \\ J, & l_1 = l_2 \neq l_3 = l_4, \\ J', & l_1 = l_4 \neq l_2 = l_3, \end{cases} \quad (5)$$

$$C_{l_1 l_2, l_3 l_4} = \begin{cases} U & l_1 = l_2 = l_3 = l_4 \\ -U' + J & l_1 = l_3 \neq l_2 = l_4, \\ 2U' - J, & l_1 = l_2 \neq l_3 = l_4, \\ J' & l_1 = l_4 \neq l_2 = l_3. \end{cases} \quad (6)$$

With these susceptibilities, the fluctuation-mediated effective interactions are obtained, which are used to calculate the self-energy. Then the renormalized Green's functions are determined self-consistently from the Dyson's equation. The obtained Green's functions and the susceptibilities are used to obtain the spin-singlet pairing interaction in the form

$$\hat{V}^s(q) = \frac{3}{2} \hat{S} \hat{\chi}_s(q) \hat{S} - \frac{1}{2} \hat{C} \hat{\chi}_c(q) \hat{C} + \frac{1}{2} (\hat{S} + \hat{C}), \quad (7)$$

and this is plugged into the linearized Eliashberg equation,

$$\begin{aligned}
 \lambda \Delta_{l'l'}(k) = & -\frac{T}{N} \sum_q \sum_{l_1 l_2 l_3 l_4} V_{l_1 l_2 l'}(q) G_{l_1 l_3}(k-q) \\
 & \times \Delta_{l_3 l_4}(k-q) G_{l_2 l_4}(q-k). \quad (8)
 \end{aligned}$$

The superconducting transition temperature,  $T_c$ , corresponds to the temperature at which the eigenvalue  $\lambda$  of the Eliashberg equation reaches unity, so that  $\lambda$  at a fixed temperature can be used as a measure for  $T_c$ . In the present calculation, the temperature is fixed at  $k_B T = 0.01$  eV, which amounts to about 100 K, and the band filling (number of electrons/site) is set to be  $n = 2.85$ , which corresponds to 0.85 electrons per site in the main band, namely, around the optimum doping

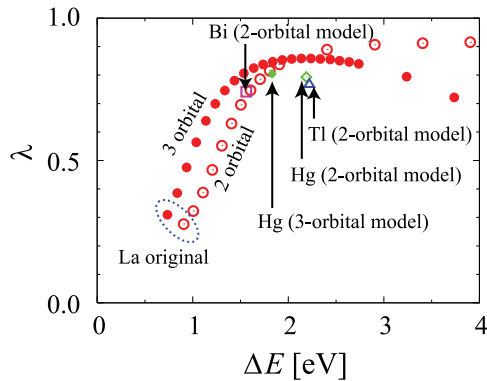


FIG. 6. (Color online) The eigenvalue,  $\lambda$ , of the Eliashberg equation for  $d$ -wave superconductivity plotted against  $\Delta E = E_{x^2-y^2} - E_{z^2}$  for the two-orbital (red open circles) and three-orbital (red solid circles) models for  $\text{La}_2\text{CuO}_4$ . Corresponding eigenvalues for  $\text{HgBa}_2\text{CuO}_4$ ,  $\text{Bi}_2\text{Sr}_2\text{CuO}_6$ , and  $\text{Tl}_2\text{Ba}_2\text{CuO}_6$  are also indicated.

concentration. We take  $32 \times 32 \times 4$   $k$ -point meshes and 1024 Matsubara frequencies.

### B. Correlation between $T_c$ and $\Delta E$

Let us now investigate how the  $d_{z^2}$  orbital affects superconductivity by hypothetically varying  $\Delta E$  from its original value of 0.91 eV (shown in Table I) to 4.0 eV for the La cuprate to single out the effect of  $\Delta E$ . The eigenvalue of the Eliashberg equation  $\lambda$  calculated as a function of  $\Delta E$  in Fig. 6 shows that  $\lambda$  initially increases rapidly upon increasing  $\Delta E$ , then saturates for  $\Delta E > 3$  eV. This means that the mixture of the  $d_{z^2}$  orbital on the Fermi surface around the wave vectors  $(\pi, 0)$ ,  $(0, \pi)$  does indeed strongly suppress superconductivity in the original La system, while for large-enough  $\Delta E$  the system essentially reduces to a single-orbital model, where the  $d_{z^2}$  orbital no longer affects superconductivity. As mentioned above, the  $d_{z^2}$  orbital mixture makes the Fermi surface more square shaped, which in itself favors superconductivity as mentioned in Sec. II A (e.g., Fig. 1 of Ref. 7). Thus, we can see that the effect of the  $d_{z^2}$  orbital mixture *supersedes* the effect of Fermi surface shape, and  $T_c$  is primarily determined by the former. This explains why we have  $T_c$  positively correlated with  $\Delta E$  simultaneously with the roundness of the Fermi surface that is also positively correlated with  $\Delta E$ . This should lead to the experimentally observed correlation between the shape of the Fermi surface and  $T_c$ .<sup>1,2</sup>

### C. Effects of the interorbital electron-electron interaction

Thus, the next important question is as follows: Why does the mixture of the  $d_{z^2}$  orbital on the Fermi surface suppress superconductivity? To investigate the origin, we have varied the interaction values to examine the strength of the spin fluctuations and the superconducting instability. The strength of the spin fluctuation is measured by the antiferromagnetic Stoner factor, which, for a multiband system, corresponds to the largest eigenvalue of the matrix  $\hat{S}\chi_0$ .

In the result in Table II we can compare the cases for  $U' = 0$  eV and  $U' = 2.4$  eV, which shows that the strength of the spin fluctuation becomes smaller when  $U'$  is turned off. This should be because  $U'$  hinders four electrons (two

TABLE II. FLEX results for the eigenvalue of the Eliashberg equation  $\lambda$ , and the Stoner factor for various values of the interorbital interactions  $U'$  and  $J$ , for fixed  $U = 3.0$  eV and  $J' = 0.30$  eV.

$U'$ (eV)	$J$ (eV)	Stoner	$\lambda$
2.4	0.3	0.979	0.279
2.4	0.0	0.978	0.335
0.0	0.3	0.925	0.291
0.0	0.0	0.958	0.309

$d_{z^2}$  and two  $d_{x^2-y^2}$ ) to come on the same site. Despite this, it can be seen that  $\lambda$  is not much affected by  $U'$ , probably because the suppression of superconductivity due to the increased charge/orbital fluctuations (which is unfavorable for singlet  $d$ -wave pairing) and the enhancement due to the increased spin fluctuations roughly cancel with each other. We have also examined how the Hund's coupling  $J$  affects superconductivity. A comparison between  $J = 0$  and  $J = 0.3$  shows that superconductivity is slightly suppressed when we turn on  $J$ , which is consistent with an observation that the Hund's coupling tends to suppress spin-singlet pairing. Nevertheless, the effect of  $J$  is overall small. The conclusion here is that the effect of the interorbital interactions on superconductivity is small, so that the main origin of the suppression of superconductivity is the mixture of the  $d_{z^2}$  orbital on the Fermi surface, which is elaborated in the next section.

### D. Origin of the suppression of superconductivity by the $d_{z^2}$ mixing

Here we pinpoint why the  $d_{z^2}$  orbital component mixture degrades  $d$ -wave superconductivity. In Fig. 7, we show the squared orbital diagonal and off-diagonal elements of the Green's function matrix spanned by the orbital indices at the lowest Matsubara frequency. We compare them for two cases: the original La cuprate and a hypothetical case where we increase  $\Delta E$  to the value for Hg, where the hopping integrals are tuned to retain the shape of the Fermi surface to that of the La cuprate. In the hypothetical case, the interaction values are reduced ( $U = 2.1$  eV,  $J = J' = 0.1U$ , and  $U' = U - 2J$ ) so as to make the maximum value of the pairing interaction in the  $d_{x^2-y^2}$  channel ( $V_{1111}$ ) to be roughly the same as that in the original La case. Then the eigenvalues of the Eliashberg equation at  $T = 0.01$  differ as much as  $\lambda = 0.28$  and 0.88 for the original La and the hypothetical cases, respectively. Let us analyze the origin of this difference. Here we denote the  $d_{x^2-y^2}$  and  $d_{z^2}$  orbitals as orbitals 1 and 2, respectively. In the original La, compared to the hypothetical case, (i) the  $d_{x^2-y^2}$  diagonal element  $|G_{11}|^2$  is smaller, especially around the wave vectors  $(\pi, 0)/(0, \pi)$ ; (ii) the  $d_{z^2}$  diagonal element  $|G_{22}|^2$  is much larger; and (iii) there is a substantial off-diagonal element  $|G_{12}|^2$  due to the strong  $d_{z^2}$  orbital mixture. If we turn to the pairing interaction matrix, again at the lowest Matsubara frequency, in Fig. 8, the diagonal elements have similar maximum values between the two cases because the interaction is reduced in the hypothetical one, as mentioned above. In the original La, the off-diagonal element of the pairing interaction  $V_{1221}$  is large compared to the hypothetical

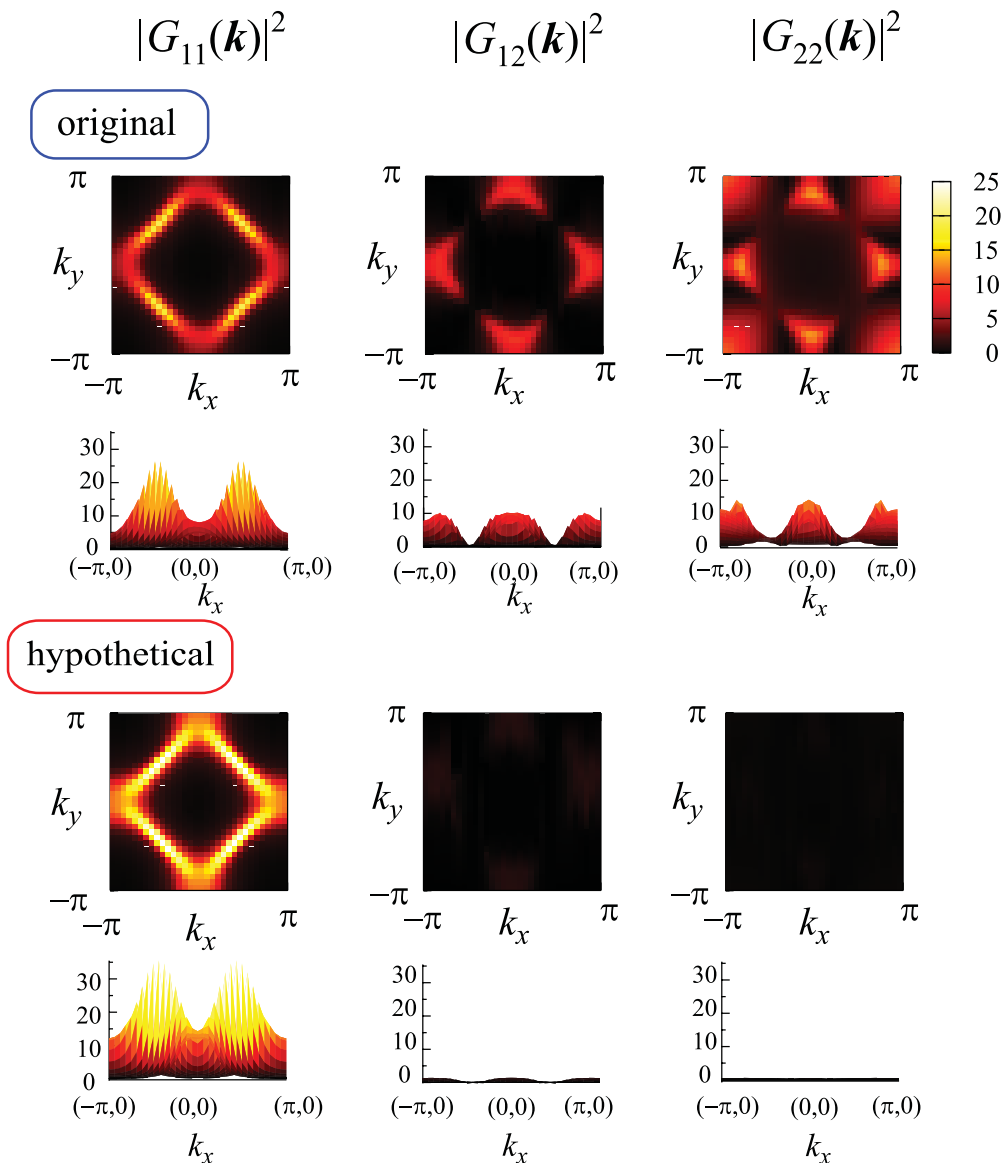


FIG. 7. (Color online) Contour plots and side views of the diagonal and off-diagonal elements of the squared Green's function for the original La and the hypothetical cases. The subscripts 1 and 2 stand for the  $d_{x^2-y^2}$  and  $d_{z^2}$  orbitals, respectively.

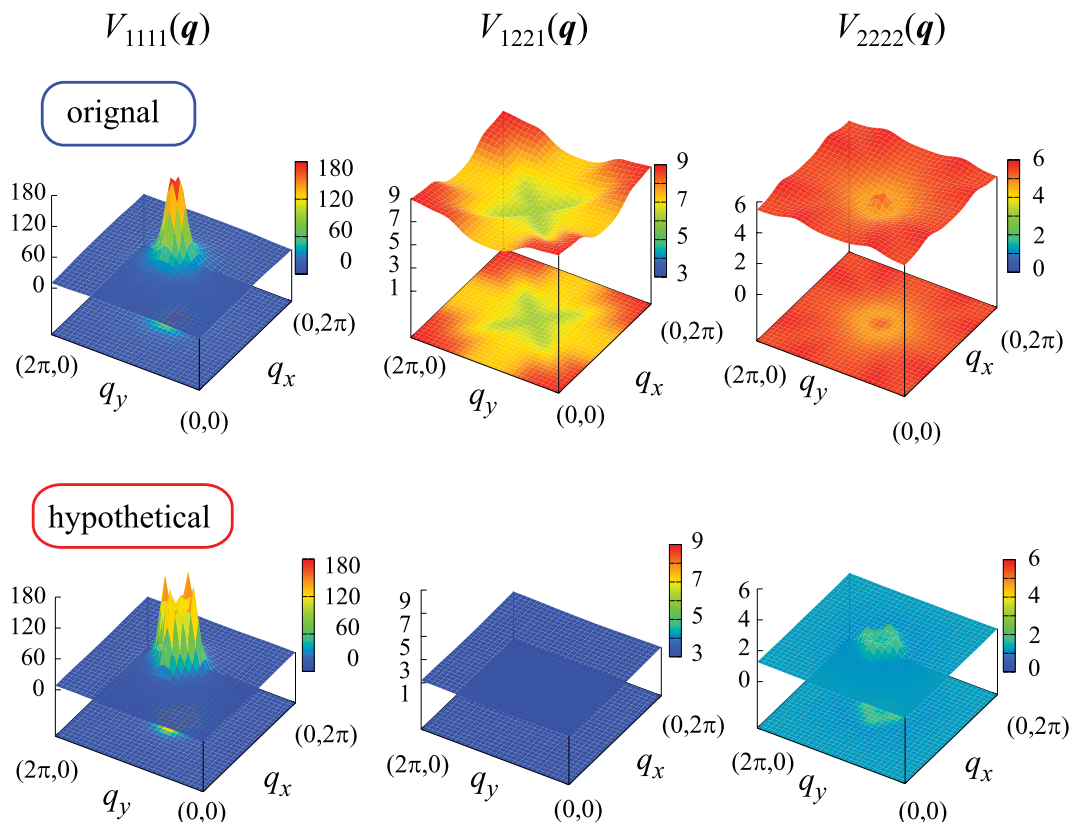
case, and the interaction is broadly peaked around  $(0,0)$ . On the other hand, the  $d_{z^2}$  diagonal interaction  $V_{2222}$  is finite but has a small momentum dependence. Considering the above, the dominant contributions to the Eliashberg equation regarding the  $d_{x^2-y^2}$  orbital component of the gap function  $\Delta_{11}$  is roughly given as

$$\begin{aligned}
 \lambda \Delta_{11}(k) \sim & -V_{1111}(\bar{Q})G_{11}(k-\bar{Q})\Delta_{11}(k-\bar{Q})G_{11}(\bar{Q}-k) \\
 & -V_{1221}(0,0)G_{21}(k)\Delta_{11}(k)G_{21}(-k) \\
 & -\sum_q V_{2222}(q)G_{22}(k-q)\Delta_{22}(k-q)G_{22}(q-k),
 \end{aligned} \tag{9}$$

where  $\bar{Q} = (\pi, \pi)$ . If we consider a wave vector  $\vec{k}$  near  $(\pi, 0)$  on the Fermi surface that has a positive  $\Delta_{11}(k)$ ,  $\Delta_{11}(k-\bar{Q})$  will be negative for the  $d$ -wave gap. Then the first term on the right-hand side will be positive but small in the original La

compared to the hypothetical case because of the small  $G_{11}$  especially around  $(\pi, 0)/(0, \pi)$ . This is the main reason why  $\lambda$  is reduced in the original La compared to the hypothetical case. In addition, the second term, which cannot be neglected when the  $d_{z^2}$  mixture is significant, actually has a negative sign, and also acts to suppress  $\lambda$  and, hence,  $T_c$ . The interaction  $V_{2222}$  has small momentum dependence, so that this term has small contribution for a  $d$ -wave gap when summed over  $q$ .

In the above comparison, we have reduced the interactions in the hypothetical case so as to make the maximum pairing interaction  $V_{1111}$  nearly the same as in the original La. The reason we fix the strength of the pairing interaction is because the maximum value of the pairing interaction actually does not differ very much upon increasing  $\Delta E$  in the results given in Fig. 6. The reason for this, despite the Fermi surface nesting becoming worse as we increase  $\Delta E$ , is mainly twofold: (i) the  $d_{z^2}$  orbital mixture on the Fermi surface becomes weaker,


 FIG. 8. (Color online) Diagonal and off-diagonal elements of the pairing interaction depicted against  $(q_x, q_y)$ .

and (ii) inclusion of the self-energy in the FLEX weakens the role of the Fermi surface nesting played in the development of the spin fluctuations. Regarding the second point, in the random phase approximation where the self-energy is not considered, the Fermi surface nesting effect on the strength of the spin fluctuations, hence the pairing interaction, is so strong that  $\lambda$  does not increase with  $\Delta E$  as in Fig. 6 (and thus the  $T_c$  difference between La and Hg cuprates discussed later cannot be explained), although the effect of the increase in  $G_{11}$  due to the reduction of the  $d_{z^2}$  mixture is present. This may be regarded as consistent with a recent result obtained with the functional renormalization group, where the self-energy correction is not considered.<sup>11</sup>

### E. $d_{x^2-y^2} + d_{z^2} + s$ three-orbital model

So far we have analyzed the two-orbital model that considers the  $d_{x^2-y^2}$  and  $d_{z^2}$  Wannier orbitals. Actually, in Refs. 23 and 1, it has been pointed out that the ‘‘axial state’’ that contains not only Cu  $d_{z^2}$  and  $O_{\text{apical}} p_z$  orbital but also the Cu 4s orbital is important in determining the shape of the Fermi surface. In the present two-orbital model, the Cu 4s orbital is effectively incorporated in both the  $d_{x^2-y^2}$  and the  $d_{z^2}$  Wannier orbitals. Namely, the Wannier orbitals have Cu 4s components in their tails. In order to examine the effect of Cu 4s orbital more explicitly, let us consider in this section a  $d_{x^2-y^2} + d_{z^2} + s$  three-orbital model which takes into account the Cu 4s Wannier orbital on an equal footing.

In this model, the 4s Wannier orbital is a mixture mainly of Cu 4s and O  $p_\sigma$  orbitals. The O  $p_\sigma$  orbitals contain not

only the in-plane  $O_{\text{plane}} p_\sigma$  but also the apical  $O_{\text{apical}} p_z$ . The main band originating from the 4s orbital for the La system is shown in the inset of Fig. 3. While the 4s band lies well ( $\approx 7$  eV) above the Fermi level, the 4s orbital still gives an important contribution to the Fermi surface shape. Here again we estimate the ratio  $(|t_2| + |t_3|)/|t_1|$  within the  $d_{x^2-y^2}$ , where we find a much smaller value of 0.10 against 0.35 in the two-orbital model. This means that the large  $t_2$  and  $t_3$  within the  $d_{x^2-y^2}$  Wannier orbital in the two-orbital model is mainly due to the  $d_{x^2-y^2} \rightarrow 4s \rightarrow d_{x^2-y^2}$  hopping path (Fig. 5, bottom panel), as pointed out in Ref. 1. Then, from the viewpoint of the three-orbital model,  $t_2$  and  $t_3$  in the single-orbital model of La cuprate are small because the  $d_{x^2-y^2} \rightarrow 4s \rightarrow d_{x^2-y^2}$  and  $d_{x^2-y^2} \rightarrow d_{z^2} \rightarrow d_{x^2-y^2}$  contributions nearly cancel with each other. The two effective hoppings have opposite signs because the  $d_{z^2}$  level lies below  $d_{x^2-y^2}$  while 4s lies above.

Now we apply FLEX to this three-orbital model, where we vary  $\Delta E = E_{x^2-y^2} - E_{d_{z^2}}$  and calculate the eigenvalue of the Eliashberg equation as we did in Sec. III B. Here we fix the on-site energy difference  $E_s - E_{d_{z^2}}$  at its original value when we vary  $\Delta E$ , because the three-orbital model for the Hg compound has roughly the same  $E_s - E_{d_{z^2}}$  as that of the La compound.

The result is displayed in Fig. 6 as marked with ‘‘3-orbital.’’ We recognize that in the small  $\Delta E$  regime the eigenvalue  $\lambda$  rapidly increases with  $\Delta E$  as in the two-orbital model. In the large  $\Delta E$  regime, however,  $\lambda$  tends to decrease rather than to saturate. In this regime, the 4s level comes too close to the Fermi level and strongly deforms the Fermi surface. Nonetheless, considering that even in the case of the

Hg compound with a larger  $\Delta E$  as is discussed later,  $\Delta E$  (three-orbital model) is still  $\simeq 2$  eV; that is, such a suppression of superconductivity due to the  $4s$  level coming too close to the Fermi level is not expected in real materials.

Thus, we can conclude on the  $4s$  orbital that, while this orbital has an important effect on the shape of the Fermi surface, the effect can be included in the two-orbital model, so that the FLEX results for the two- and three-orbital models are similar as far as the  $T_c - \Delta E$  relation is concerned (unless we consider unrealistically large  $\Delta E$ ). This is natural in that the level offset  $E_{x^2-y^2} - E_{z^2}$  is smaller ( $\simeq 1$  eV) than the electron-electron interaction ( $\simeq 3$  eV), while the  $E_s - E_{x^2-y^2}$  is much larger ( $\simeq 7$  eV). Hence, the  $4s$  orbital can effectively be integrated out before the many-body analysis, while the

$d_{z^2}$  orbital cannot. In this sense the two-orbital ( $d_{x^2-y^2} - d_{z^2}$ ) model suffices for discussing the material dependence of the  $T_c$  in the cuprates.

#### IV. MATERIAL DEPENDENCE OF $\Delta E$

We have seen that the mixture of the  $d_{z^2}$  component strongly affects superconductivity, making  $T_c$  positively correlated with  $\Delta E$ . To further endorse this, we have plotted in Fig. 6 the eigenvalue  $\lambda$  for the two-orbital models for single-layered cuprates  $\text{Bi}_2\text{Sr}_2\text{CuO}_6$ ,<sup>29</sup>  $\text{Tl}_2\text{Ba}_2\text{CuO}_6$ ,<sup>30</sup> and  $\text{HgBa}_2\text{CuO}_4$  as well, whose lattice structures are shown in Fig. 9. We can see that these materials also fall upon reasonably well on the correlation between  $\lambda$  and  $\Delta E$ . Thus, the next fundamental question in understanding the material dependence of  $T_c$  is which key factors determine  $\Delta E$ . This section precisely addresses that question.

##### A. Crystal-field effect

Since the main components of the Wannier orbitals in the two-orbital model are the Cu  $3d_{x^2-y^2}$  and Cu  $3d_{z^2}$  orbitals, the crystal-field splitting between these orbitals, denoted as  $\Delta E_d$  here, should be the first key factor governing  $\Delta E$ . Namely, materials with a larger apical oxygen height above the  $\text{CuO}_2$  plane ( $h_O$ ) should have a larger crystal-field splitting,<sup>20</sup> so that  $\Delta E_d$ , and thus  $\Delta E$ , should be larger (Fig. 4). Indeed, the La compound has smaller  $h_O = 2.41$  Å and  $\Delta E$ , while the Hg compound has larger  $h_O = 2.78$  Å and  $\Delta E$ .

So let us first focus on how the apical oxygen height  $h_O$  affects  $\Delta E_d$ . Namely, we construct a model that considers all of the Cu  $3d$  and O  $2p$  orbitals (five  $3d + 3 \times 4 2p = 17$  orbitals) explicitly, exploiting maximally localized Wannier orbitals, and then estimate the on-site energy difference between Cu  $d_{x^2-y^2}$  and Cu  $d_{z^2}$  orbitals as  $\Delta E_d$ . We note that this  $\Delta E_d$  is something different from  $\Delta E$  defined for the effective two-orbital model we have considered, since we now explicitly consider the oxygen  $2p$  orbitals. In Fig. 10, we plot  $\Delta E_d$  as a function of  $h_O$ , where we hypothetically vary the height for the La system from its original value 2.41 to 2.90 Å. The result shows that  $\Delta E_d$  and  $h_O$  are linearly correlated. We have also constructed similar  $d$ - $p$  models for the Bi, Tl, and Hg systems, and we can see that the  $\Delta E_d$  values for

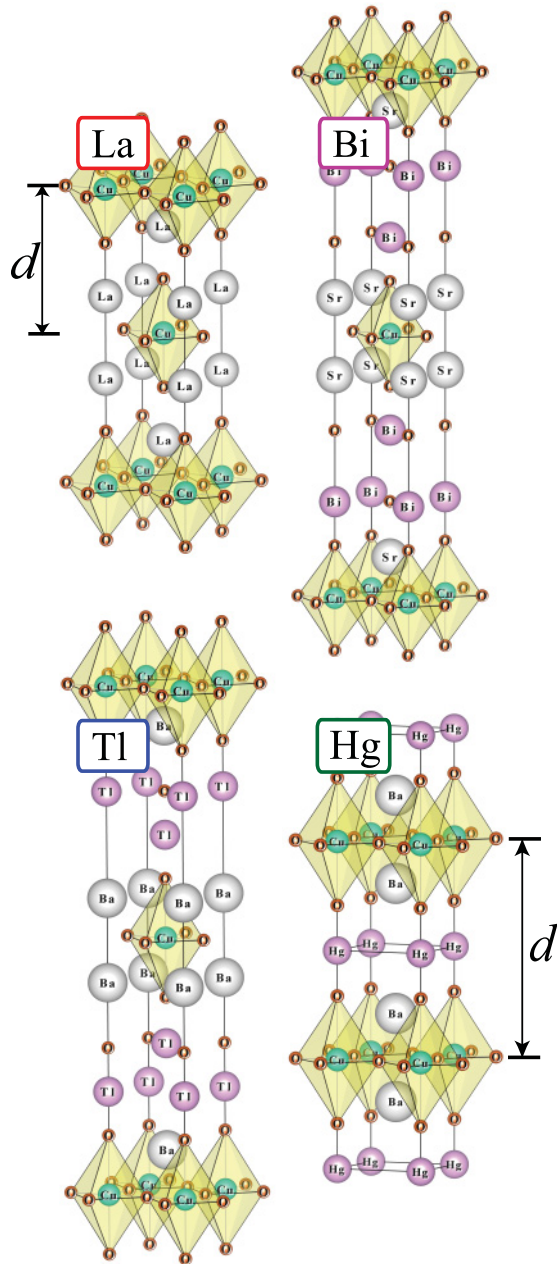


FIG. 9. (Color online) Lattice structures of  $\text{La}_2\text{CuO}_4$ ,  $\text{Bi}_2\text{Sr}_2\text{CuO}_6$ ,  $\text{Tl}_2\text{Ba}_2\text{CuO}_6$ , and  $\text{HgBa}_2\text{CuO}_4$ .

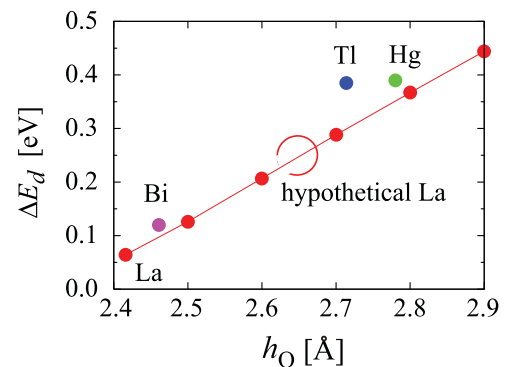


FIG. 10. (Color online)  $\Delta E_d$  plotted against  $h_O$ . Solid (red) circles connected by a line represent the result for the hypothetical lattice structure of La cuprate, while values for Bi, Tl, and Hg cuprates are also shown.

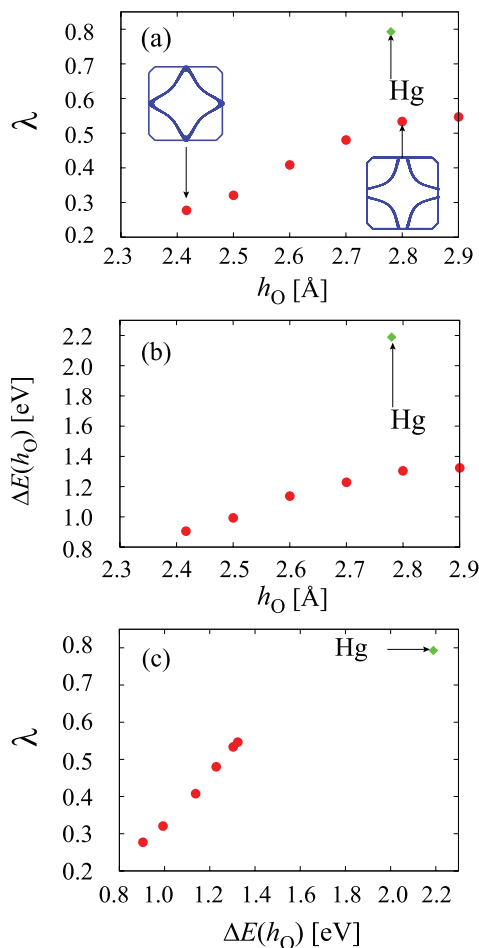


FIG. 11. (Color online) The eigenvalue of the Eliashberg equation  $\lambda$  (circles) when  $h_O$  is varied (a) or  $\Delta E(h_O)$  is varied (c) hypothetically in the lattice structure of La cuprate. Also plotted is  $\Delta E(h_O)$  against  $h_O$  (b). Diamonds in green indicate the values for HgBa<sub>2</sub>CuO<sub>4</sub>.

these materials, also included in the figure, roughly fall upon the linear correlation for the hypothetical La system, which indicates that  $\Delta E_d$  is primarily determined by  $h_O$ . Such a correlation has also been found in a recent quantum chemical calculation,<sup>10</sup> where the  $d_{x^2-y^2}-d_{z^2}$  level splitting evaluated there corresponds more closely to the present  $\Delta E_d$  rather than  $\Delta E$ .

Having seen that  $h_O$  governs  $\Delta E_d$ , we next look at  $\Delta E$  and the eigenvalue  $\lambda$  in the two-orbital models for the La cuprate with hypothetically varied  $h_O$ . As expected,  $\Delta E$  in Fig. 11(b) monotonically increases with  $h_O$ . Then  $\lambda$  [Fig. 11(a)] increases with  $h_O$ , which is in accord with the positive correlation between  $\Delta E$  and  $\lambda$  discussed above [Fig. 11(c)]. Thus,  $h_O$  is shown to be one of the key parameters that determine  $\Delta E$  and thus  $T_c$ .

However, if we plot the corresponding values for the Hg cuprate, also displayed in the figure, we find that  $\Delta E$ , and thus  $\lambda$ , are larger than those for the hypothetical La cuprate for the same apical oxygen height between the two cuprates. This implies that  $h_O$  and  $\Delta E_d$  are not the sole parameters that determine  $\Delta E$  and hence  $T_c$ , and another factor should be lurking.

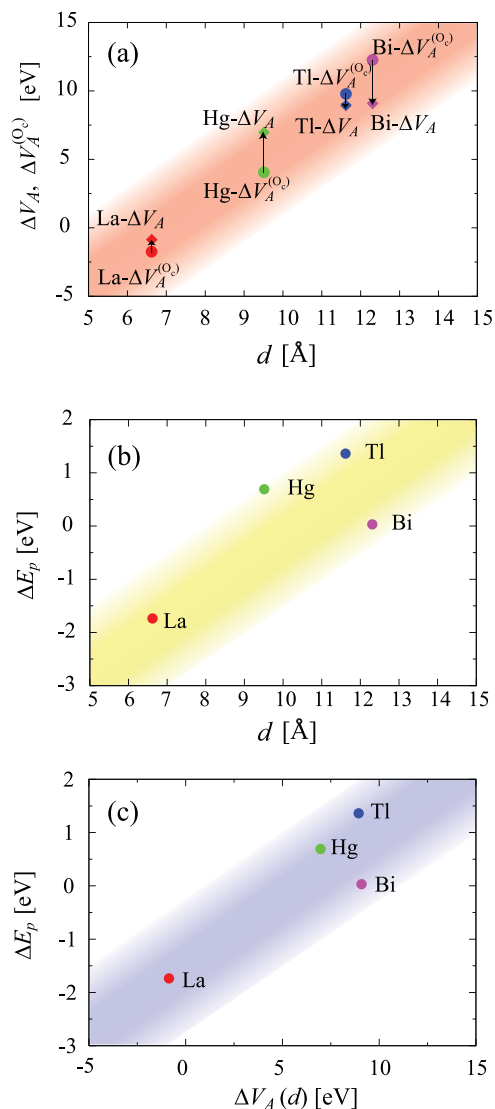


FIG. 12. (Color online) (a)  $\Delta V_A^{(O_c)}$  (circles) and  $\Delta V_A$  (diamonds) plotted against the layer separation  $d$  for La, Bi, Hg, and Tl cuprates. (b) The level offset,  $\Delta E_p$ , between the in-plane  $p_\sigma$  and the apical oxygen  $p_z$  against the layer separation  $d$ . (c) The correlation between  $\Delta V_A$  and  $\Delta E_p$ .

## B. Oxygen-orbital effects

The above observation has motivated us to look more closely into the effects of oxygen orbitals. As shown in Fig. 4, the Wannier orbitals in our two-orbital model, the Cu- $3d_{x^2-y^2}$  and  $3d_{z^2}$  orbitals, strongly hybridize with the in-plane O  $2p_\sigma$  and apical oxygen O  $2p_z$  orbitals, respectively. Thus, we can surmise that  $\Delta E$  should also be affected by the energy difference (denoted as  $\Delta E_p$ ) between the in-plane  $p_\sigma$  and the apical oxygen  $p_z$ . By definition, one can expect that  $\Delta E_p$  is positively correlated with  $\Delta V_A$ , the Madlung potential difference between O<sub>plane</sub> and O<sub>apical</sub> introduced by Ohta *et al.* as an important parameter that controls the material dependence of the  $T_c$ .<sup>31</sup> In fact,  $\Delta V_A$  for Hg is about 7 eV larger than that of La, namely, the O- $2p_z$  energy level is much lower in Hg.

The difference mainly comes from the crystal structure where the apical oxygen in the La cuprate is surrounded by other apical oxygens belonging to the neighboring layers, while in Hg those oxygen atoms are much further apart, as seen in Fig. 9. This gives a clue to understanding the reason why the hypothetical La cuprate with the same  $h_O$  as Hg has smaller  $\Delta E$  and  $\lambda$ ; although  $\Delta E_d$  is similar between the two systems,  $\Delta E_p$  very much differs. Thus, the difference between La and Hg can be attributed to the distance between neighboring  $\text{CuO}_2$  layers that is affected by the lattice structure, that is, body-centered tetragonal (bct) vs simple tetragonal. However, a similar variance in the layer distance can occur even within similar lattice structures. La, Bi, and Tl compounds all have the bct structures, so naively one might expect similar values of  $\Delta V_A$ . However,  $\Delta V_A$ 's for Bi and Tl are much larger than that for La. This is because in Bi (Tl) there is a Bi-O (Tl-O) layer inserted between the adjacent  $\text{CuO}_2$  layers (see Fig. 9), resulting in a large  $\text{CuO}_2$  layer separation.

So let us focus on the separation between the neighboring  $\text{CuO}_2$  planes, which will be denoted as  $d$  here. Figure 12(a) plots  $\Delta V_A^{(\text{O}_c)}$  against  $d$  for La, Hg, Tl, and Bi cuprates. Here we have defined  $\Delta V_A^{(\text{O}_c)}$  as the contribution to  $\Delta V_A$  coming from the apical oxygens. These Madelung potentials are calculated by placing point charges at atomic positions, as was done in Ref. 31. We have also plotted the total  $\Delta V_A$  for the four materials, which indicates that  $\Delta V_A$  is roughly governed by  $\Delta V_A^{(\text{O}_c)}$ , which in turn is mainly determined by  $d$ . We also plot  $\Delta E_p$  against  $d$  in Fig. 12(b) for the four cuprates. Here again,  $\Delta E_p$  is obtained using the model that considers the Cu  $3d$  and O  $2p$  orbitals explicitly. From these we can see that both  $\Delta V_A$  and  $\Delta E_p$  are primarily correlated positively with the layer separation  $d$ . This, in turn, implies that  $\Delta E_p$  and  $\Delta V_A$  in Fig. 12(c) are positively correlated as well.

### C. Classification of materials by $\Delta E_d$ and $\Delta E_p$

We have seen that  $\Delta E_d$  and  $\Delta E_p$  are mainly determined by  $h_O$  and  $d$ , respectively. Combining these, we can summarize the dependence of  $\Delta E$  on the material and lattice structure as

$$\Delta E \simeq f(\Delta E_d(h_O), \Delta E_p(d)), \quad (10)$$

where  $f$  is a certain function. For instance, La and Bi have smaller  $\Delta E_d$  reflecting smaller  $h_O$ , while Hg and Tl have larger  $\Delta E_d$  due to larger  $h_O$ . Namely, the latter group tends to have larger  $\Delta E$ . On the other hand, Bi, Tl, and Hg have larger  $d$  than La, so that they have larger  $\Delta V_A$ . We can summarize all these into a classification of materials in terms of  $\Delta E_d$  and  $\Delta E_p$  as a numerical Table III and a kind of ‘‘phase diagram’’

TABLE III. The values of  $\Delta E_d$  (along with  $h_O$ ),  $\Delta E_p$  (along with  $d$ ), and  $\Delta E$  for La, Bi, Hg, and Tl cuprates.

	La	Bi	Hg	Tl
$\Delta E_d$ (eV)	0.064	0.12	0.39	0.39
$h_O$ (Å)	2.41	2.46	2.78	2.71
$\Delta E_p$ (eV)	-1.7	0.030	0.89	1.4
$d$ (Å)	6.6	12.3	9.5	11.6
$\Delta E$ (eV)	0.91	1.6	2.2	2.2

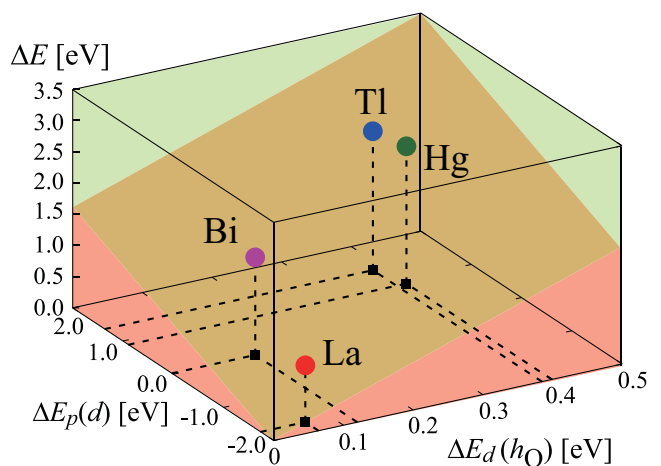


FIG. 13. (Color online)  $\Delta E$  plotted against  $\Delta E_p$  and  $\Delta E_d$  for the four single-layered cuprates considered here. An oblique plane indicates a rough correlation between  $\Delta E$  and  $(\Delta E_p, \Delta E_d)$ .

in Fig. 13. Apart from the effect of  $h_O$  (or  $\Delta E_d$ ),  $\Delta E$  is positively correlated with  $\Delta E_p$  and thus with  $\Delta V_A$ , so that  $\Delta V_A$  and  $T_c$  should be roughly correlated. In this sense, the so-called Maekawa’s plot (Fig. 2 of Ref. 31) is consistent with the present Fig. 6. Also, a negative correlation between the occupancy of holes with  $p_z - d_{z^2}$  character and  $T_c$  has been found in Ref. 22, which is again consistent with the present view.

## V. DISCUSSIONS

### A. Validity of the present model

In the present study, we have adopted the LDA to derive the kinetic-energy part of the model Hamiltonian. The LDA calculation neglects some of the electron correlation effects, and our standpoint in the present study is that the remaining part of the electron correlation is dealt with in the FLEX calculation. One might suspect, however, that there might remain electron correlation effects that are not taken into account in the present approach but can affect the accuracy of the evaluation of the level offset  $\Delta E$  between  $d_{x^2-y^2}$  and  $d_{z^2}$  Wannier orbitals. Our view on this point is the following. First, it is an experimental fact that the La cuprate has a squarelike Fermi surface, while the Bi cuprate a rounded one.<sup>2</sup> This is accurately reproduced in the LDA, which strongly suggests that the  $d_{z^2}$  component is indeed strongly mixed around  $(\pi, 0), (0, \pi)$ , that is,  $\Delta E$  is small, in the La cuprate. Second, a detailed quantitative difference in  $\Delta E$  will not affect the present conclusions. To see this, we have performed an LDA +  $U$  calculation to obtain the kinetic-energy part of the Hamiltonian, varying  $U$  from 0 to 6 eV. For La, the considerable  $d_{z^2}$  character around  $(\pi, 0), (0, \pi)$  persists even at  $U = 6$ , and the band that intersects the Fermi level is only slightly changed, although  $\Delta E$  somewhat increases with  $U$ . On the other hand, for Hg  $\Delta E$  is greatly enhanced by  $U$ , but this does not significantly affect the  $d_{x^2-y^2}$  main band, since the  $d_{z^2}$  character is already absent at  $U = 0$ . Applying FLEX to these LDA +  $U$  models will result in a double counting of the electron correlation effects because FLEX takes account of the first-order terms, but if we took, for the sake of comparison,

the obtained  $\Delta E$ , we would find that a considerable difference in  $\lambda$  between La ( $\lambda \simeq 0.5$ ) and Hg ( $\simeq 0.8$ ) is still present even if we adopt the modified values of  $\Delta E$ .

### B. Possibility of higher- $T_c$ materials

A consequence of our study is that superconductivity in the single-layered cuprates is optimized when the system has a single-band nature. In such a case (as in Hg cuprate), the Fermi surface is rounded due to the effect of the Cu  $4s$  orbital. As mentioned in Sec. II A, the square-shaped Fermi surface would be more favorable for superconductivity for single-orbital systems. For this very reason, even the HgBa<sub>2</sub>CuO<sub>4+ $\delta$</sub>  is not fully optimized as a single-layered material. Indeed, the hypothetical La cuprate having a large  $\Delta E$  but with a Fermi surface similar to that in the original La gives a larger  $\lambda$  in the Eliashberg equation as we have seen in Sec. III D. So we have a bit of a dilemma, since it would be difficult to get rid of the effect of the Cu  $4s$  orbital *as far as the cuprates are concerned*. Conversely, however, we can seek for other materials in which the  $4s$  orbital is not effective. An example is a single-band system consisting of  $d_{xy}$  orbitals, where the hybridization between  $d_{xy}$  and  $4s$  orbitals is forbidden by symmetry. In fact, a possible way of realizing a single-band  $d_{xy}$  system has been proposed in Ref. 32. Provided that such a system has the band width and the electron-electron interaction strength similar to those in the cuprates (since too strong or too weak a correlation will degrade superconductivity), it can possibly give even higher  $T_c$ .

## VI. CONCLUSION

To summarize, we have studied a two-orbital model that considers both  $d_{x^2-y^2}$  and  $d_{z^2}$  Wannier orbitals in order to

pinpoint the key factors governing the material dependence of  $T_c$  within the single-layered cuprates. We conclude that the  $d_{z^2}$  orbital mixture on the Fermi surface is significantly degrades superconductivity. Since the energy difference  $\Delta E$  between the  $d_{x^2-y^2}$  and the  $d_{z^2}$  governs the mixture as well as the shape of the Fermi surface, we identify  $\Delta E$  as the key parameter in the material dependence of  $T_c$  in the cuprates. Since the mixing effect supersedes the effect of the Fermi surface nesting, a small  $\Delta E$  results in a suppression of  $T_c$  despite a square-shaped Fermi surface.  $\Delta E$  is then shown to be determined by the energy difference  $\Delta E_d$  between the two Cu  $3d$  orbitals, and the energy difference  $\Delta E_p$  between the O<sub>plane</sub>  $p_\sigma$  and O<sub>apical</sub>  $p_z$ , both of which are affected by the lattice structure.  $\Delta E_d$  is a crystal field splitting, which is mainly determined by the apical oxygen height, while  $\Delta E_p$  is found to be primarily governed by the interlayer separation  $d$ . The materials that have highest  $T_c$ 's within the single-layered cuprates, Hg and Tl systems, indeed have  $\Delta E$  large enough to make them essentially single-band. On the other hand, there is still room for improvement if we can suppress the effect of the Cu  $4s$  mixing that makes the Fermi surface rounded, which may be realized in noncuprate materials with  $U$  similar to the cuprates in magnitude.

## ACKNOWLEDGMENTS

We are grateful to O. K. Andersen and D. J. Scalapino for fruitful discussions. The numerical calculations were performed at the Supercomputer Center, ISSP, University of Tokyo. This study has been supported by Grants-in-Aid for Scientific Research from JSPS (Grants No. 23340095, R.A.; No. 23009446, H.S.; No. 21008306, H.U.; and No. 22340093, K.K. and H.A.). H.S. and H.U. acknowledge support from JSPS. R.A. thanks JST-PRESTO for financial support.

- 
- <sup>1</sup>E. Pavarini, I. Dasgupta, T. Saha-Dasgupta, O. Jepsen, and O. K. Andersen, *Phys. Rev. Lett.* **87**, 047003 (2001).
- <sup>2</sup>K. Tanaka, T. Yoshida, A. Fujimori, D. H. Lu, Z.-X. Shen, X.-J. Zhou, H. Eisaki, Z. Hussain, S. Uchida, Y. Aiura, K. Ono, T. Sugaya, T. Mizuno, and I. Terasaki, *Phys. Rev. B* **70**, 092503 (2004).
- <sup>3</sup>T. Moriya and K. Ueda, *J. Phys. Soc. Jpn.* **63**, 1871 (1994).
- <sup>4</sup>C. T. Shih, T. K. Lee, R. Eder, C.-Y. Mou, and Y. C. Chen, *Phys. Rev. Lett.* **92**, 227002 (2004).
- <sup>5</sup>P. Prelovšek and A. Ramšak, *Phys. Rev. B* **72**, 012510 (2005).
- <sup>6</sup>For a review, see, e.g., D. J. Scalapino, in *Handbook of High Temperature Superconductivity*, edited by J. R. Schrieffer and J. S. Brooks (Springer, New York, 2007), Chap. 13.
- <sup>7</sup>H. Sakakibara, H. Usui, K. Kuroki, R. Arita, and H. Aoki, *Phys. Rev. Lett.* **105**, 057003 (2010).
- <sup>8</sup>C. Weber, K. Haule, and G. Kotliar, *Phys. Rev. B* **82**, 125107 (2010).
- <sup>9</sup>X. Wang, H. T. Dang, and A. J. Millis, *Phys. Rev. B* **84**, 014530 (2011).
- <sup>10</sup>L. Hozoi, L. Siurakshina, P. Fulde, and J. van den Brink, *Nat. Sci. Rep.* **1**, 65 (2011).
- <sup>11</sup>S. Uebelacker and C. Honerkamp, e-print [arXiv:1111.1171](https://arxiv.org/abs/1111.1171) (to be published).
- <sup>12</sup>P. Blaha, K. Schwarz, G. K. H. Madsen, D. Kvasnicka, and J. Luitz, *Wien2k: An Augmented Plane Wave + Local Orbitals Program for Calculating Crystal Properties* (Vienna University of Technology, Wien, 2001).
- <sup>13</sup>J. D. Jorgensen, H.-B. Schüttler, D. G. Hinks, D. W. Capone II, K. Zang, M. B. Brodsky, and D. J. Scalapino, *Phys. Rev. Lett.* **58**, 1024 (1987).
- <sup>14</sup>J. L. Wanger, P. G. Radaelli, D. G. Hinks, J. D. Jorgensen, J. F. Mitchell, B. Dabrowski, G. S. Knapp, and M. A. Beno, *Physica C* **201**, 447 (1993).
- <sup>15</sup>N. E. Bickers, D. J. Scalapino, and S. R. White, *Phys. Rev. Lett.* **62**, 961 (1989).
- <sup>16</sup>T. Dahm and L. Tewordt, *Phys. Rev. Lett.* **74**, 793 (1995).
- <sup>17</sup>Th. Maier, M. Jarrell, Th. Pruschke, and J. Keller, *Phys. Rev. Lett.* **85**, 1524 (2000).
- <sup>18</sup>P. R. C. Kent, T. Saha-Dasgupta, O. Jepsen, O. K. Andersen, A. Macridin, T. A. Maier, M. Jarrell, and T. C. Schulthess, *Phys. Rev. B* **78**, 035132 (2008).
- <sup>19</sup>K. Shiraishi, A. Oshiyama, N. Shima, T. Nakayama, and H. Kamimura, *Solid State Commun.* **66**, 629 (1988).
- <sup>20</sup>H. Kamimura and M. Eto, *J. Phys. Soc. Jpn.* **59**, 3053 (1990); M. Eto and H. Kamimura, *ibid.* **60**, 2311 (1991).
- <sup>21</sup>A. J. Freeman and J. Yu, *Physica B* **150**, 50 (1988).

- <sup>22</sup>C. Di Castro, L. F. Feiner, and M. Grilli, *Phys. Rev. Lett.* **66**, 3209 (1991).
- <sup>23</sup>O. K. Andersen, A. I. Liechtenstein, O. Jepsen, and F. Paulsen, *J. Phys. Chem. Solids* **56**, 1573 (1995).
- <sup>24</sup>S. Baroni *et al.* [<http://www.pwscf.org/>]. Here we take the exchange correlation functional introduced by J. P. Perdew, K. Burke, and Y. Wang, [*Phys. Rev. B* **54**, 16533 (1996)], and the wave functions are expanded by plane waves up to a cutoff energy of 60 Ry with  $20^3k$ -point meshes.
- <sup>25</sup>J. Kunes, R. Arita, P. Wissgott, A. Toschi, H. Ikeda, and K. Held, *Comput. Phys. Commun.* **181**, 1888 (2010).
- <sup>26</sup>N. Marzari and D. Vanderbilt, *Phys. Rev. B* **56**, 12847 (1997); I. Souza, N. Marzari, and D. Vanderbilt, *ibid.* **65**, 035109 (2001). The Wannier functions are generated by the code developed by A. A. Mostofi, J. R. Yates, N. Marzari, I. Souza, and D. Vanderbilt [<http://www.wannier.org/>].
- <sup>27</sup>The conclusion of the present study is not sensitive to the choice of the interaction values. For instance, if we raise the interactions to  $U = 4.5$  eV ( $\sim 10t$ ) and  $J = 0.45$  eV, the eigenvalue of the Eliashberg equation for the two-orbital model discussed in Fig. 6 is only slightly modified to  $\lambda = 0.29$  for La and 0.72 for Hg.
- <sup>28</sup>K. Yada and H. Kontani, *J. Phys. Soc. Jpn.* **74**, 2161 (2005).
- <sup>29</sup>We have adopted the lattice parameter of Bi compound from H. Sawa, H. Fujiki, K. Tomimoto, and J. Akimitsu, *Jpn. J. Appl. Phys.* **27**, L830 (1988).
- <sup>30</sup>We adopted the lattice parameter of Tl compound from C. C. Torardi, M. A. Subramanian, J. C. Calabrese, J. Gopalakrishnan, E. M. McCarron, K. J. Morrissey, T. R. Askew, R. B. Flippen, U. Chowdhry, and A. W. Sleight, *Phys. Rev. B* **38**, 225 (1988).
- <sup>31</sup>Y. Ohta, T. Tohyama, and S. Maekawa, *Phys. Rev. B* **43**, 2968 (1991).
- <sup>32</sup>R. Arita, A. Yamasaki, K. Held, J. Matsuno, and K. Kuroki, *Phys. Rev. B* **75**, 174521 (2007).